

Use of diffusion-weighted magnetic resonance imaging (DW-MRI) to investigate the effect of chemoradiotherapy on the salivary glands

PATRICIA DOORNAERT¹, MAX DAHELE¹, REDINA LJUMANOVIC², REMCO DE BREE³, BEN J. SLOTMAN¹ & JONAS A. CASTELIJNS²

¹Department of Radiation Oncology, VU University Medical Center, Amsterdam, The Netherlands,

²Department of Radiology and Nuclear Medicine, VU University Medical Center, Amsterdam, The Netherlands

and ³Department of Otolaryngology and Head and Neck Surgery, VU University Medical Center, Amsterdam, The Netherlands

To the Editor,

Chemoradiotherapy (CRT) is the standard treatment for locally advanced head and neck cancer (HNC), offering comparable survival to surgery with the benefit of organ preservation. However, one of the most troublesome side effects is parotid (PG) and submandibular gland (SMG) toxicity leading to loss of gland function and hypo-salivation. The mechanism of salivary gland toxicity is incompletely understood and interventions for preventing or reversing hypo-salivation are currently limited [1]. The use of intensity-modulated radiotherapy (IMRT) to reduce salivary gland dose is now routine, but it is only partially effective [2,3]. Non-invasive imaging might help to better understand the response of the glands to CRT and identify salivary gland toxicity. This could in turn help to develop therapeutic strategies. A previous report suggested that diffusion-weighted magnetic resonance imaging (DW-MRI) before and after treatment might be a promising tool for investigating changes due to

radiotherapy [4]. Our goal was to image the effect of CRT on salivary glands using DW-MRI performed before, during and after CRT. Although DW-MRI in HNC is often performed with echo planar imaging (EPI) sequences, this technique is particularly prone to geometric distortions due to susceptibility artefacts. To overcome these possible disadvantages, we also used a non-EPI technique, (half-fourier acquisition single-shot turbo spin-echo, HASTE) [5]. Taking into account work that suggests heterogenous effects of radiation within glands, and different responses in PG and SMG, we analyzed sub-regions within individual glands and evaluated the parotid and submandibular glands separately [6–8]. We also looked for correlations between DW-MRI changes and planned radiation dose. In comparison with previous literature, the use of two different DW-MRI sequences, analysis of sub-regions in the glands and availability of imaging during, as well as before and after CRT, are strengths of this study.

Material and methods

Patients

The present report describes an analysis of imaging data from a prospective institutional study investigating DW-MRI and tumor control [9]. All patients had combined modality treatment for locally advanced HNC: seven patients had an oropharynx and one patient a hypopharynx carcinoma; four had cisplatin-based CRT, two had cetuximab-based CRT and two had induction-chemotherapy with cetuximab and TPF (docetaxel, cisplatin, 5-fluorouracil) followed by cisplatin-based CRT. MRI scans made on the same scanner (1.5 Tesla Sonata, Siemens, Erlangen, Germany) were available for eight patients before and during CRT, and 5/8 patients after CRT (three patients had post-treatment scans on another machine and were not analyzed).

Radiotherapy

All patients had a contrast enhanced planning computed tomography (CT) scan (2.5 mm slice thickness) in an immobilization mask. Dose prescription was either 54.25 Gy (1.55 Gy/fraction; $n = 2$) or 57.75 Gy (1.65 Gy/fraction; $n = 6$) to the elective regions and 70 Gy (2 Gy/fraction) to the primary tumor delivered as a simultaneous integrated boost. Treatment planning was performed using the Eclipse™ treatment planning system (Varian Medical Systems, Palo Alto, CA, USA).

MRI examinations

The baseline MRI scans (DW-MRI₁) were made before the start of chemotherapy and radiotherapy (range 0–24 days before RT, 102–114 days before RT in patients receiving induction CT). A second DW-MRI (DW-MRI₂) was performed after the

delivery of 20 ($n = 7$) or 22 ($n = 1$) Gy to the tumor, and a third MRI examination (DW-MRI₃), available in five patients, was made 2–3 months (70–91 days) after completion of therapy. For all examinations, a head coil combined with a phased array spine and neck coil was used and axial MR images were acquired (22 slices with 4 mm slice thickness), centered on the primary tumor and enlarged nodes. EPI parameters were: TR/TE = 5000/105 ms, in-plane pixel size = 2×2 mm, and b-values = 0, 500 and 1000 s/mm² (three averages). Parameters for HASTE were: TR/TE = 900/110 ms, in-plane pixel size = 1.1×1.1 mm, and b-values = 0 s/mm² (three averages) and 1000 s/mm² (12 averages). The ADC maps were calculated using the software of the MRI machine (units of 10^{-5} mm²/s).

Regions of interest (ROIs) within salivary glands

Ten 7 mm diameter spherical ROIs were defined for each patient on the planning CT scan: three in each PG (upper part, lower part and deep lobe) and two in each SMG (anterior and posterior). For each patient a diagram of the ROI location was generated. Using this diagram, a corresponding ROI was drawn on each of the DW-MRIs and the ADC value was recorded.

Analysis

In this small study, only simple descriptive statistics were used.

Results

The pooled data for all ROIs is summarized in Table I. In the five patients with DW-MRI data after treatment, the mean dose to the entire ipsilateral (IL) and contralateral (CL) PG was 43.9 Gy (± 6 Gy

Table I. Radiation (RT) doses and ADC values for EPI and HASTE DW-MRI before, during and after treatment for different regions of interest (ROI) in the ipsilateral (IL) and contralateral (CL) parotid (PG) and submandibular glands (SMG). Values presented as mean (standard deviation).

ROI	Baseline ($n = 8$)		During ($n = 8$)		RT dose ^b	After ($n = 5$)			
	HASTE ADC ^a	EPI ADC	HASTE ADC	EPI ADC		HASTE ADC	EPI ADC	RT dose	
IL PG	upper	67 (28)	76 (20)	60 (16)	76 (31)	6.0 (3.3)	97	111 (13)	21.1 (7.6)
	lower	76 (22)	96 (16)	82 (15)	115 (23)	14.7 (4.0)	100 (26)	136 (10)	53.8 (16.1)
	deep	78 (22)	89 (11)	73 (12)	100 (35)	18.7 (1.8)	106 (25)	125 (16)	67.5 (5.9)
CL PG	upper	68 (22)	77 (21)	61 (24)	66 (30)	2.9 (0.9)	85 (31)	106 (25)	11.8 (2.0)
	lower	73 (19)	87 (14)	73 (20)	112 (23)	10.1 (4.9)	100 (31)	125 (27)	38.4 (19.8)
	deep	76 (25)	88 (15)	77 (19)	99 (31)	13.9 (5.8)	105 (37)	117 (26)	54.2 (20.6)
IL SMG	anterior	82 (26)	110 (13)	99 (15)	135 (14)	18.4 (3.2)	125 (26)	152 (13)	66.9 (8.4)
	posterior	80 (24)	107 (13)	100 (18)	133 (11)	20.4 (1.3)	125 (25)	151 (11)	72.8 (1.0)
CL SMG	anterior	83 (29)	108 (15)	97 (20)	129 (12)	14.7 (7.0)	120 (24)	147 (10)	62.7 (5.1)
	posterior	81 (27)	109 (11)	99 (21)	132 (11)	18.0 (2.9)	118 (17)	144 (11)	67.5 (5.9)

^aADC values in units of $\times 10^{-5}$ mm²/s; ^bRT dose in Grays.

standard deviation, SD) and 31.4 Gy (± 6.6 Gy SD), respectively. The SMGs received a mean dose of 59.4–73.2 Gy. The mean dose to the upper PG was the lowest of all ROIs: 6.0 Gy (IL) and 2.9 Gy (CL) after approximately two weeks of CRT, and 21.1 Gy (IL) and 11.8 Gy (CL) after the completion of treatment. In all time periods, EPI and HASTE ADC values were lower for the PG than the SMG. When comparing the PG ROIs, in all time periods, including prior to treatment, there was a difference in ADC results for both EPI and HASTE imaging, with the lower and deep ROIs having higher ADC values than the upper ROIs.

During treatment

When all PG and SMG ROIs were taken together, both EPI and HASTE ADC values were higher after approximately two weeks of treatment than at baseline (mean 94 before treatment vs. 111 during treatment for EPI, and 76 before treatment vs. 83 during treatment for HASTE). When considering PG and SMG ROIs separately, the rise in ADC values for both PG and SMG was most noticeable using EPI DW-MRI (PG: mean 84 before treatment vs. 95 during treatment and for SMG: mean 109 before treatment vs. 132 during treatment). Considering all ROIs together, the correlation between the dose received early in treatment and the change (Δ) in ADC (Spearman's rank coefficient) was $r = 0.23$ for EPI and $r = 0.38$ for HASTE.

After treatment

For the combined PG and SMG ROIs there was an increase in EPI and HASTE ADC values after treatment compared with baseline (mean 94 before treatment vs. 131 after treatment with EPI, and 75 before treatment vs. 108 after treatment with HASTE; Table I). Taking all ROIs together, the correlation between the total dose received by the ROI and Δ ADC for the HASTE technique was $r = 0.33$, and $r = 0.11$ for the EPI technique (Figure 1).

Discussion

Two different DW-MRI techniques were used to explore changes in the salivary glands approximately two weeks into and three months after CRT for head and neck cancer. Both MRI techniques showed a rise in PG and SMG ADC during and after CRT. ADC values with both EPI and HASTE were lower in the PG than the SMG and with both techniques there appeared to be regional differences within the PG and SMG. HASTE showed a better correlation between dose and Δ ADC between baseline and during/after CRT.

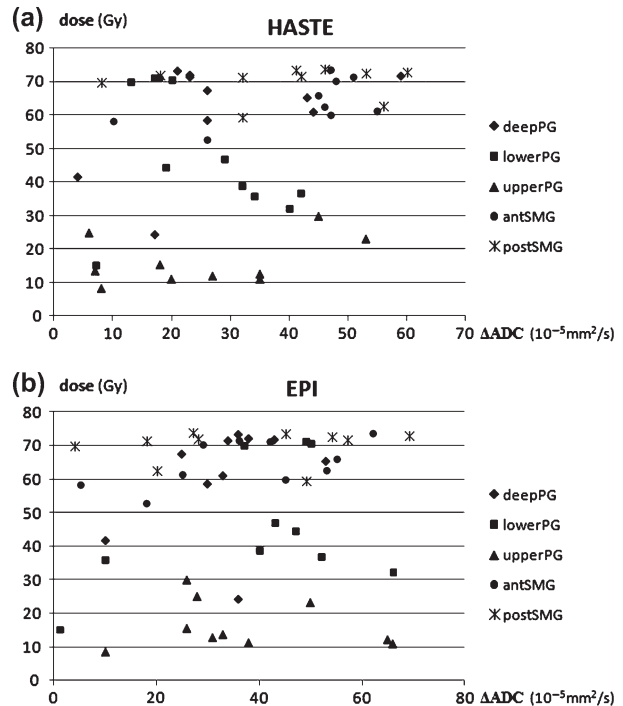


Figure 1. (a). Change in HASTE DW-MRI ADC values 3 months after therapy versus radiotherapy dose. Spearman's rank coefficient for all ROIs together 0.33. (b). Change in EPI DW-MRI ADC values 3 months after therapy versus radiotherapy dose. Spearman's rank coefficient for all ROIs together 0.11.

We observed an increase in all PG and SMG ADC values after CRT and found no difference between IL and CL ADC values. This is in contrast to Dirix et al. [8], who found a significant difference in whole gland ADC values before and six months after RT in the IL, but not in the CL PG. This could be due to the fact that the dose difference between the IL and CL PG was much larger in the series from Dirix (33.9 Gy vs. 12.5 Gy) and our post-treatment imaging may be too soon after treatment [7].

Several limitations of this study should be mentioned, including the following: 1) The most apparent is the small sample size, which prevented more detailed statistical analysis; 2) There were differences in treatment schedule and chemotherapy/biological agents; 3) There were differences in scan timing; 4) Whole gland data was not available in all patients due to an inadequate scan trajectory (the scans were originally performed for tumor analysis); 5) Clinical/physiological data is not available to correlate with the DW-MRI changes; 6) We have used planned dose, rather than the estimated actual delivered dose that would take into account deformation and volume change in the PG and SMG as a result of treatment; and 7) DW-MRI is subject to geometric distortion, hampering co-localization of the ROIs on the planning CT and the MRI studies.

Nonetheless, despite these limitations, we have been able to make several observations, including

that: salivary gland ADC values rose during and after treatment with both EPI and HASTE DW-MRI techniques and differences between/within the PG and SMG were observed. In addition, we have observed that different DW-MRI techniques may provide different data. This suggests that while DW-MRI merits further investigation as a marker of CRT effect in the salivary glands: the optimum DW-MRI technique and timing needs to be defined, glands should be considered separately and sub-regions within the glands should be analyzed. More detailed understanding of possible heterogeneity in the response to CRT within an individual gland and the relationship between radiotherapy dose and functional effect could help to support the development of sophisticated treatment planning with preferential sparing of specific parts of the salivary glands, in an effort to further reduce the morbidity of CRT [<http://clinicaltrials.gov/show/NCT01955239>].

Declaration of interest: The authors report no conflicts of interest. The authors alone are responsible for the content and writing of the paper.

References

- [1] Vissink A, van Luijk P, Langendijk J, Coppes R. Current ideas to reduce or salvage radiation damage to salivary glands. *Oral Dis Epub* 2014 Feb 28.
 - [2] Doornaert P, Verbakel WF, Rietveld DH, Slotman BJ, Senan S. Sparing the contralateral submandibular gland without compromising PTV coverage by using volumetric modulated arc therapy. *Radiat Oncol* 2011;6:74.
 - [3] Nutting CM, Morden JP, Harrington KJ, Urbano TG, Bhide SA, Clark C, et al. PARSPORT trial management group. Parotid-sparing intensity modulated versus conventional radiotherapy in head and neck cancer (PARSPORT): A phase 3 multicentre randomised controlled trial. *Lancet Oncol* 2011;12:127–36.
 - [4] Dirix P, De Keyzer F, Vandecaveye V, Stroobants S, Hermans R, Nuyts S. Diffusion-weighted magnetic resonance imaging to evaluate major salivary gland function before and after radiotherapy. *Int J Radiat Oncol Biol Phys* 2008;71:1365–71.
 - [5] Verhappen MH, Pouwels PJ, Ljumanovic R, van der Putten L, Knol DL, De Bree R, et al. Diffusion-weighted MR imaging in head and neck cancer: Comparison between half-fourier acquired single-shot turbo spin-echo and EPI techniques. *AJNR Am J Neuroradiol* 2012;33:1239–46.
 - [6] Konings AW, Cotteleer F, Faber H, van Luijk P, Meertens H, Coppes RP. Volume effects and region-dependent radiosensitivity of the parotid gland. *Int J Radiat Oncol Biol Phys* 2005;62:1090–5.
 - [7] Coppes RP, Vissink A, Konings AW. Comparison of radiosensitivity of rat parotid and submandibular glands after different radiation schedules. *Radiother Oncol* 2002;63:321–8.
 - [8] Teshima K, Murakami R, Yoshida R, Nakayama H, Hiraki A, Hirai T, et al. Histopathological changes in parotid and submandibular glands of patients treated with preoperative chemoradiation therapy for oral cancer. *J Radiat Res* 2012;53:492–6.
 - [9] Schouten CS, de Bree R, van der Putten L, Noij DP, Hoekstra OS, Comans EF, et al. Diffusion-weighted EPI- and HASTE-MRI and 18F-FDG-PET-CT early during chemoradiotherapy in advanced head and neck cancer. *Quant Imaging Med Surg* 2014;4:239–50.
-